Micromechanical Characterization of LPSO Phase in Mg-Zn-Y Alloys

Kazuki Takashima[1], Masaaki Otsu[2]

[1]Kumamoto University; 2-39-1 Kurokami; Kumamoto 860-8555, Japan
[2]Fukui University; 3-9-1 Bunkyo; Fukui 910-8507, Japan

Keywords: Mg-Zn-Y alloy, LPSO phase, Fracture, Crack growth

Abstract

A microfracture testing technique was used to examine the fracture properties of a long-period stacking ordered (LPSO) phase in Mg-Zn-Y alloys. Micro-sized cantilever specimens composed of the LPSO phase with dimensions of 10 × 20 × 50 μm^3 were selectively prepared from a $Mg_{88}Zn_5Y_7$ alloy by focused ion beam (FIB) machining. Further, notches with a width of 0.5 μm and a depth of 5 μm were introduced into the micro-sized specimens. Microfracture tests were performed on the micro-sized specimens using a mechanical testing machine. The fracture toughness values (K_Q) of the LPSO phase were 1.2–3.0 MPam$^{1/2}$. Transmission electron microscopy (TEM) observation indicated that the K_Q values were dependent on crack orientation in the LPSO phase, and higher K_Q values were obtained when crack propagation was parallel to the c-axis of the LPSO phase. This suggests that controlling LPSO phase orientation effectively improves fracture toughness in Mg-Zn-Y alloys.

Introduction

Mg-Zn-Y alloys that contain a long-period stacking ordered (LPSO) phase exhibit high strength and good ductility as compared to conventional Mg alloys [1]. Mg-Zn-Y alloys consist of an α-Mg phase and an 18R LPSO phase [2] and their mechanical properties have been found to be enhanced by hot extrusion. Their excellent mechanical properties are thought to originate from grain refinement of the α-Mg matrix and kink bands formed during hot extrusion in the LPSO phase [3, 4]; however, the details of this contribution have not yet been determined. Therefore, it is important to investigate the mechanical properties of the LPSO phase to determine the fundamental strengthening mechanism of this alloy system. In particular, the fracture properties of these alloys, including fracture toughness, are essential for their practical application to structural components. It is important to know the fracture properties of each constituent phase of two-phase materials such as Mg-Zn-Y alloys (the α-Mg phase and LPSO phase in the Mg-Zn-Y alloy). However, it is rather difficult to examine the fracture properties of each phase by conventional fracture testing, as their sizes are in the order of several tens of microns.

We have developed a microscale fracture testing technique, and have measured the fracture properties of specimens with dimensions of 10–50 μm [5]. The specimen size in this testing technique was smaller than that of each constituent of the Mg-Zn-Y alloy. The fracture properties of the LPSO phase in Mg-Zn-Y alloys can be directly evaluated if micro-sized specimens are prepared and microscale fracture tests are performed.

In this investigation, the fracture toughness and fracture behavior of the LPSO phase in Mg-Zn-Y alloys were examined using the microscale fracture testing technique.

Experimental Procedure

The material used was $Mg_{88}Zn_5Y_7$ alloy. This material was hot-extruded with an extrusion ratio of 10 at 723 K. Figures 1(a) and (b) show scanning electron micrographs of the micro-structure of this alloy from the different cross sections of the extruded bar. The LPSO phase is elongated in the extrusion direction. The volume fraction of the LPSO phase in this alloy is approximately 80%,

and the grain size is approximately 30–50 μm; hence, it is possible to prepare LPSO single-phase micro-sized specimens.

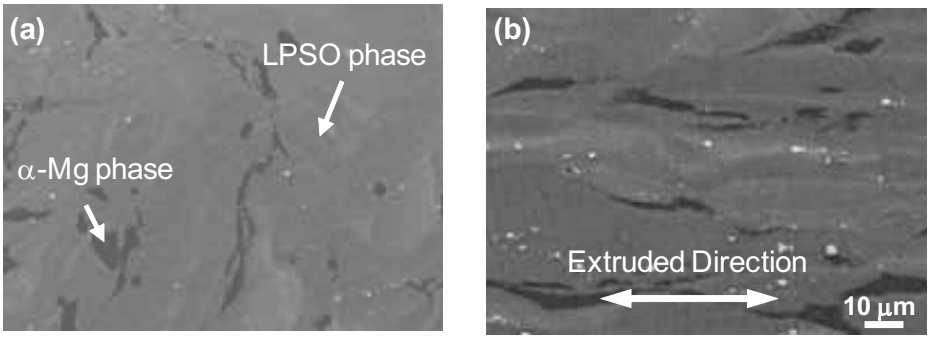

Figure 1. Microstructure of extruded $Mg_{88}Zn_5Y_7$ alloy. (a) Vertical cross section, (b) Longitudinal cross section of the rod.

Micro-sized specimens were prepared and cut from the extruded bar vertical and parallel to the extrusion direction (hereafter referred to as Type-V and Type-P specimens, respectively). These slices were polished on both sides to form approximately 20 μm thick foils. Micro-sized cantilever beam specimens were prepared using focused ion beam (FIB) machining. Figure 2 shows a scanning electron micrograph of a micro-sized specimen. The length (L), breadth (B), and thickness (W) of the specimens were 50, ~20, and 10 μm, respectively.

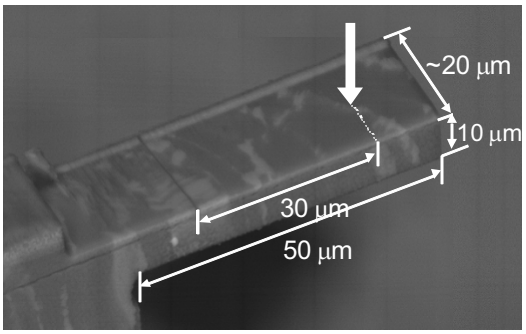

Figure 2. Scanning electron micrograph of micro-sized specimen prepared from $Mg_{88}Zn_5Y_7$ alloy.

The loading position was located 40 μm from the fixed end of the specimen. Notches with a width of 0.5 μm and depth of 3.5–5 μm were also introduced into the micro-sized specimens using FIB machining. The notch position was set 10 μm from the fixed end of the specimen. Fracture tests were carried out using a mechanical testing machine for micro-sized materials, which was developed in our laboratory. The load resolution and displacement resolution of the testing machine were 20 μN and 0.2 nm, respectively. The loading position was adjusted using an accurate X–Y stage at a translation resolution of 0.05 μm.

After the fracture tests were conducted, the fracture surfaces were observed using scanning electron microscopy (SEM). In addition, the sample for transmission electron microscopy (TEM) was prepared from a fractured specimen using FIB, and the microstructures and crystalline orientations of the crack paths were observed.

Experimental Results and Discussion

Fracture Properties

Figure 3 shows the load–displacement curves during fracture tests of the micro-sized specimens. The difference in the maximum load is attributed to the size of the specimens, which were prepared by hand polishing, and the length of the notches, whose depths were difficult to control by FIB machining. Fractures occurred in a brittle manner for both Type-P and Type-V specimens. Therefore, it is assumed that cracks began to propagate at the maximum load.

The K_Q values were calculated from the maximum load and by using the following equations for stress intensity (K) for a notched cantilever beam [6].

$$K = \frac{6PS}{W^2 B}\sqrt{\pi a}F(a/W) \tag{1}$$

where

$$F(a/W) = 1.122 - 1.40\,(a/W) + 7.33\,(a/W)^2 - 13.08\,(a/W)^3 + 14.0(a/W)^4 \tag{2}$$

In equation (1), a, P, and S are the total crack length, failure load, and the distance between the loading point and the notch position, respectively. The failure load (P_Q) was thought to be the maximum load of the load–displacement curve. After the tests were conducted, the notch length (a) was measured from the SEM observation of the fracture surface.

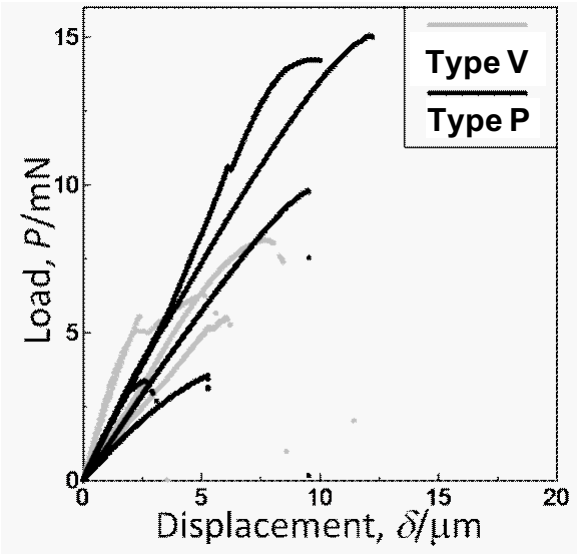

Figure 3. Load-displacement curves obtained during fracture toughness testing of $Mg_{88}Zn_5Y_7$ alloy.

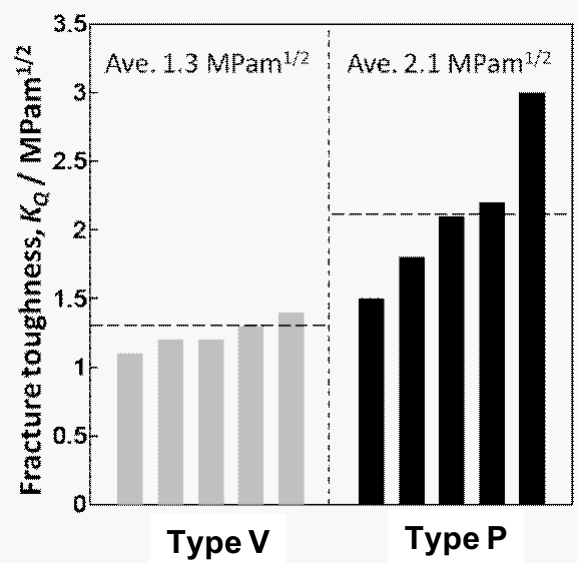

Figure 4. Fracture toughness values obtained by fracture testing of $Mg_{88}Zn_5Y_7$ alloy.

As the K_Q values do not satisfy the small-scale yielding conditions in this study, provisional K_Q values were considered. Calculated fracture toughness values for the types of specimens are shown in Figure 4. The fracture toughness values of the Type-V specimen are 1.2–1.3 MPam$^{1/2}$, and those of the Type-P specimen are 1.4–3.0 MPam$^{1/2}$. The K_Q value of the Type-P specimen is higher than that of the Type-V specimen.

Fracture Surfaces and Crack Paths

Figures 5 (a) and (b) show scanning electron micrographs of the fracture surface after fracture tests. The fracture surface of the Type-V specimen had cleavage-like facets, as shown in Figure 5 (a). In contrast, the fracture surface of the Type-P specimen had many asperities, as shown in Figure 5 (b). This indicates that the fracture mechanisms of the Type-V and Type-P specimens are different. This also suggests anisotropy of the LPSO phase fracture. This material has a strong basal plane texture because of the extrusion process [7]. The differences in fracture toughness may be due to crystallographic orientation variations in the LPSO phase.

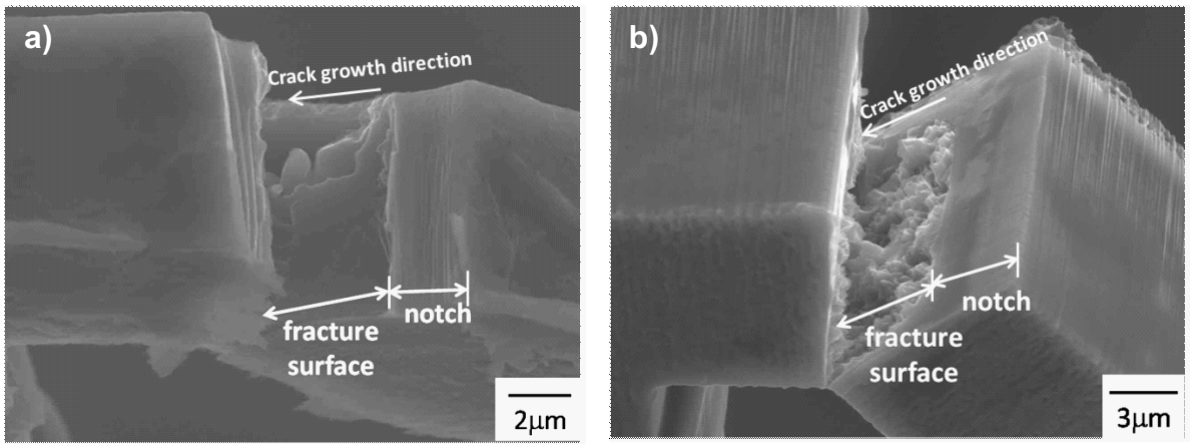

Figure 5. Scanning electron micrograph of LPSO micro-sized specimens after fracture testing. (a) Type-V specimen, (b) Type-P specimen

In order to investigate the relation between crack growth and crystallographic orientation, TEM samples were prepared from the centers of the specimens using FIB, and TEM observations were made for the two types of specimens.

Figure 6 shows the crack path of the Type-V specimen (K_Q = 1.3 MPam$^{1/2}$) observed by TEM. Figure 6 (a) shows straight crack propagation when the c-axis is perpendicular to the direction of crack growth. On the other hand, Figure 6 (b) shows that the crack bends when the c-axis is parallel to the direction of crack growth. Figure 7 shows the crack path of the Type-P specimen (K_Q = 3.0 MPam$^{1/2}$) observed by TEM. The black and white contrasts following the crack path are the deposition and amorphous layers, respectively, for the TEM sample prepared by FIB. Figures 7 (a) and (b) show that the crack propagation is parallel to the c-axis. Fracture toughness when the crack propagation is parallel to the c-axis is higher than the fracture toughness when the crack propagation is perpendicular to the c-axis.

These results suggest that the fracture properties of the Mg-Zn-Y alloy can be improved by controlling the LPSO phase orientation.

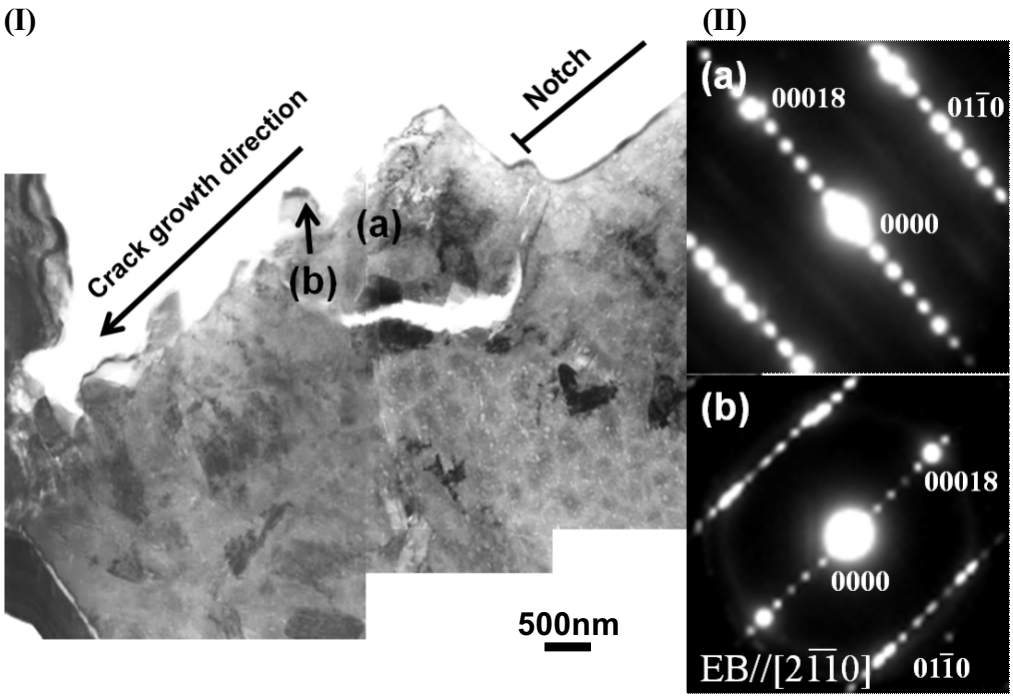

Figure 6. (I) Bright field image of crack path in Type-V specimen and (II) (a), (b) Electron diffraction pattern selected by (a) and (b) in image (I).

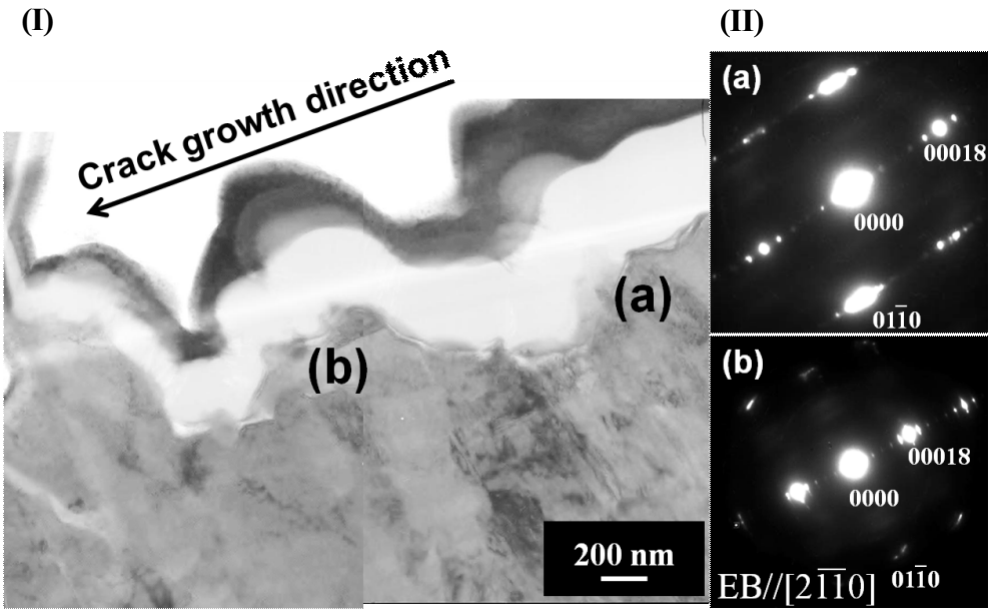

Figure 7. (I) Bright field image of Crack Path in Type-P specimen and (II) (a), (b) Electron diffraction pattern selected by (a) and (b) in image (I).

Conclusions

A micro-sized testing technique was applied for investigating the fracture properties of the LPSO phase in an Mg-Zn-Y alloy and the following conclusions were obtained:

(1) Fracturing occurred in a brittle manner and anisotropy in fracture toughness was observed depending on the direction of crack growth.

(2) Cracks tend to propagate along the (0001) plane of the LPSO phase, and crack initiation and growth resistance were higher in the [0001] direction. This resulted in the anisotropy in fracture toughness.

(3) LPSO phase morphology and orientation affect crack growth resistance, suggesting that the fracture properties of Mg-Zn-Y alloys can be improved by controlling the morphology and orientation of the LPSO phase.

References

[1] Y. Kawamura et al., "Rapidly Solidified Powder Metallurgy $Mg_{97}Zn_1Y_2$ Alloys with Excellent Tensile Yield Strength above 600 MPa", *Materials Transactions*, 42 (2001), 1172- 1176.

[2] T. Morikawa et al., "The Fine-Grained Structure in Magnesium Alloy Containing Long-Period Stacking Order Phase", *Materials Transactions*, 49 (2008), 1294-1297.

[3] S. Yoshimoto, M. Yamasaki, and Y. Kawamura, "Microstructure and Mechanical Properties of Extruded Mg-Zn-Y Alloys with 14H Long Period Ordered Structure", *Materials Transactions*, 47 (2006), 959-965.

[4] Y. Kawamura, and M. Yamasaki, "Formation and Mechanical Properties of $Mg_{97}Zn_1RE_2$ Alloys with Long-Period Stacking Ordered Structure", *Materials Transactions*, 48 (2007), 2986- 2992.

[5] K. Takashima, and Y. Higo, "Fatigue and Fracture of a Ni-P Amorphous Alloy Thin Film on the Micrometer Scale", *Fatigue and Fracture of Engineering Materials and Structures*, 28 (2005), 703-710.

[6] H. Okamura, *Introduction to Linear Fracture Mechanics*, (Baifukan, Tokyo, 1976), p. 218.

[7] T. Yamaguchi, K. Saito, and Y. Kawamura, "Investigation of Strengthening Mechanism in Extrusion of $Mg_{96}Zn_2Y_2$ Alloy Ingot and Chips", *Journal of Japan Institute of Light Metals*, 57 (2007), 571-577.